Janilee Y. Benitez graduated from the University of California, Berkeley with a B.A. in anthropology and an emphasis in archaeology in 2005. She completed the B.S. physics major requirements at California State University, East Bay in 2007. During her undergraduate career, she held an internship at the University of California, San Diego's Research Experience for Undergraduates (REU) program, and a second internship at Lawrence Berkeley National Lab's (LBNL) SULI program. She continues to work with her mentor Daniela Leitner at LBNL and plans to attend graduate school to earn a PhD in either Nuclear Physics or Nuclear Engineering.

Daniela Leitner got her PhD in experimental physics from the University of Technology in Vienna, Austria, in 1995. Her thesis was focused on aspects to advance the Li plasma edge diagnostic technique used on fusion reactor experiments. In 1996 she was awarded with the "Schrödinger Fellowship" administered by the Austrian Academy of Science to conduct the research project "Development of multiply-charged ion sources" at the Lawrence Berkeley National Laboratory. This research project led to the design and construction of a compact ECR ion source, which was used for the online production of radioactive ion beams, resulting in record intensities of low energy ^{14}O ion beams (consequently used for a precision measurement of the ^{14}O lifetime). After completion of her fellowship year she joined the Lawrence Berkeley National Laboratory, where she has been working as a staff scientist since 2000 and was promoted to senior scientist in 2006. Currently she is heading the accelerator physics and ECR ion source development group at the 88-Inch Cyclotron. This group has designed and built the next generation superconducting ECR ion source VENUS, which is presently the most advanced ECR ion source worldwide. Under her lead, the 88-Inch accelerator physics group is currently working on the development of advanced simulation tools to model the transport of multi species heavy ion beams extracted from ECR ion sources.

Analysis of X-Ray Spectra Emitted from the VENUS ECR Ion Source

Janilee Benitez, Daniela Leitner

ABSTRACT

The Versatile Electron Cyclotron resonance ion source for Nuclear Science (VENUS), located at Lawrence Berkeley National Lab's 88-inch cyclotron, extracts ion beams from a plasma created by ionizing a gas with energetic electrons. Liquid-helium cooled superconducting coils produce magnetic fields that confine the plasma and high microwave frequencies heat the electrons enough to allow for successive ionizations of the neutral gas atoms. The combination of strong plasma confinement and high microwave frequencies results in VENUS' production of record breaking ion beam currents and high charge state distributions. While in operation, VENUS produces significant quantities of bremsstrahlung, in the form of x-rays, primarily through two processes: 1) electron-ion collisions within the plasma, and 2) electrons are lost from the plasma, collide with the plasma chamber wall, and radiate bremsstrahlung due to their sudden deceleration. The bremsstrahlung deposited into the plasma chamber wall is absorbed by the cold mass used to maintain superconductivity in the magnets and poses an additional heat load on the cryostat. In order for VENUS to reach its maximum operating potential of 10 kW of 28 GHz microwave heating frequency, the heat load posed by the emitted bremsstrahlung must be understood. In addition, studying the bremsstrahlung under various conditions will help further our understanding of the dynamics within the plasma. A code has been written, using the Python programming language, to analyze the recorded bremsstrahlung spectra emitted from the extraction end of VENUS. The code outputs a spectral temperature, which is relatively indicative of the temperature of the hot electrons, and total integrated count number corresponding to each spectra. Bremsstrahlung spectra are analyzed and compared by varying two parameters: 1) the heating frequency, 18 GHz and 28 GHz, and 2) the ratio between the minimum magnetic field and the resonant magnetic field, .44 and .70, at the electron resonant zone.

Introduction

The Versatile Electron Cyclotron resonance ion source for Nuclear Science (VENUS), located at Lawrence Berkeley National Laboratory's 88-inch cyclotron, is the most advanced superconducting ion source capable of using high frequencies and high magnetic fields to produce a plasma from which ion beams are extracted [1,2]. The capability VENUS has to produce high charge state ion beams at record intensities makes it a vital instrument in nuclear science research. Ion beams, like the ones produced by VENUS, are used to conduct research in various realms such as astrophysics, heavy elements and nuclear chemistry studies, and weak interactions. Fully understanding its production mechanisms will allow it to be run at its maximum potential and should be done before its ion beams can be used as a source for such research.

Most Electron Cyclotron Resonance (ECR) ion sources, including VENUS, rely on the superposition of solenoid and sextupole magnetic fields for plasma confinement. VENUS, in particular, has a strong plasma confinement since its magnetic fields are produced using liquid-helium cooled superconducting coils. The plasma electrons are resonantly heated up to several hundred keV using microwave heating. In VENUS, the electron heating is done using 18 GHz energy, produced by a klystron, or 28 GHz energy, produced by a gyrotron, or dual frequency 18

and 28 GHz heating. Heating occurs as the free electrons absorb the microwave energy. When the electrons have gained enough energy, through microwave heating, they are capable of ionizing by impact. Plasma ions are created through a step by step ionization process involving collisions with the electrons. In addition to the bremsstrahlung produced via electron-ion collisions, electrons that are not perfectly confined in the plasma will collide with the wall producing bremsstrahlung in the form of x-rays due to their sudden deceleration. High energy x-rays can penetrate the plasma chamber wall and be partially absorbed by the liquid helium surrounding the coils. The cryogenics system can remove only a limited amount of the heat from the cryostat. If more heat is added to the system than can be removed, the temperature of the liquid helium rises and can cause the superconducting coils to quench. The heating induced into the cryostat by the absorption of the x-rays can reach several W/kW. However the cryostat cooling system can only dissipate up to 3 W. Therefore, careful attention must be given to the amount of heat posed by the emitted bremsstrahlung before VENUS is run at its maximum operating potential of 10 kW at 28 GHz.

As a result of previous studies of the VENUS emitted bremsstrahlung, modifications have already been made to the plasma chamber. A plasma chamber surrounded by 2mm of Ta shielding was designed and implemented, and this reduced the bremsstrahlung heat load by a factor of 10. However, the 2 mm of Ta becomes transparent for x-rays with energies above 300 keV [2]. Data presented in this paper shows that under certain conditions the bremsstrahlung far surpasses 600 keV where the 2 mm of tantalum provide no shielding. The energy spectrum of the emitted bremsstrahlung is indicative of the energy of the electrons within the plasma and, as such, can reveal a lot of information about the plasma's properties, which are yet to be fully understood.

This paper presents studies done on the axially emitted bremsstrahlung. The bremsstrahlung spectra and their spectral temperatures, which are used as a relative indication of the temperature of the electron energy distribution function [3], are compared for different source parameters. In particular, microwave power input, magnetic mirror configuration and confinement, and resonant frequency heating are varied. Conclusions regarding their effect on the electron heating are presented.

Materials and Methods

Electron Heating in VENUS

The combination of three superconducting axial coils and six superconducting radial coils surrounding the plasma chamber in the VENUS design produce a plasma containment zone composed of axial fields of up to 4T at injection and 3T at extraction, and radial fields increasing radially outward everywhere to 2T at the chamber wall. The superposition of the magnetic fields produced by the three superconducting axial coils, an injection, middle, and extraction solenoid, form the magnetic mirror structure. The magnetic mirror structure shown in Figure 1a, characterized by the values B_{INJ}, B_{MIN}, and B_{EXT} that create the desired confinement structure, is of particular interest in this study. For the data presented, the current through the three axial coils (at injection, center and extraction) was varied to create the desired axial magnetic field in the center of the source (B_{MIN}) as shown in Figure 6 while keeping the mirror peak fields

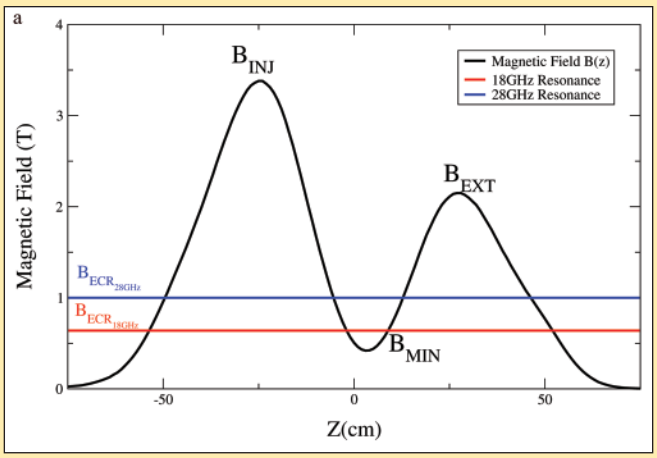

Figure 1. (a) The magnetic mirror structure that helps to contain the plasma is created by the three superconductive coils surrounding the VENUS plasma chamber. The magnetic mirror structure is characterized by the values B_{INJ}, B_{MIN}, and B_{EXT}. **(b)** A simple schematic of the experimental setup is shown. The axially emitted bremsstrahlung first passes through collimator 1, approximately 2.4 m after the extraction end of VENUS. The bremsstrahlung is collimated a second time through collimator 2 immediately before reaching the NaI photodetector. For the combined bremsstrahlung and radioactive source spectra, the radioactive source is placed directly before collimator 2 as shown above. The total extraction-detection distance is approximately 4.6 m.

(B_{INJ} and B_{EXT}) constant (see Figure 1a). Also varied were the heating frequency and the power input at each heating frequency.

The electron's Larmor frequency is shown in Equation 1:

$$B_{ECR} = \frac{m_{e^-}\omega}{Q_{e^-}} \quad (1)$$

where Q_{e^-} is the electron charge, m_{e^-} is the electron mass, and ω is the microwave heating frequency. Since VENUS uses 18 GHz or 28 GHz heating frequencies the electron resonant magnetic fields, $B_{ECR_{18GHz}}$ or $B_{ECR_{28GHz}}$, according to Equation 1, are 0.64 T or 1 T, respectively, and are also shown in Figure 1a. In other words, as the electrons spiral along the magnetic field lines in the magnetic mirror structure, when they encounter the resonant magnetic field they can absorb energy and be heated. The heating of electrons is necessary in order to ionize atoms and multiply ionize ions through collisions. The recorded axially emitted bremsstrahlung spectra primarily results from these ionizing collisions as well as electron collisions with the chamber wall.

Bremsstrahlung Spectra Collection

The experimental set-up of the VENUS source and NaI detector is shown in Figure 1b. The ions are extracted from the plasma at an extraction energy of approximately 20 keV and transported through

the analyzing magnet, after which the charge state distribution of the ion species are measured. The x-ray radiation is observed axially through the straight port of the analyzing magnet and collimated by Collimator 1 about 2.4 m after the extraction aperture of the plasma chamber, with which it is carefully aligned. Collimator 1 has an acceptance angle of 0.2 degrees which represents a 14 mm diameter at the extraction aperture. Since the extraction aperture is only 8 mm, we are also detecting bremsstrahlung from electron collisions with the plasma chamber extraction wall. Collimator 2 follows Collimator 1 by about 2 m. The sodium iodide (NaI) detector used to detect the bremsstrahlung is placed directly behind Collimator 2. In sum, the axially emitted bremsstrahlung is measured approximately 4.6 m after the extraction aperture of the ion source.

The NaI detector is comprised of a 3x3 inch NaI scintillator and a photomultiplier tube. In order to avoid detecting background radiation, the NaI detector is surrounded by lead bricks. The NaI scintillator absorbs the incident bremsstrahlung and, in turn, emits photons proportional to the deposited energy. Each emitted photon is collected by the photomultiplier which converts it into an electrical pulse and amplifies it through a series of stages. Finally, the amplified pulse is recorded by a multi-channel analyzer (MCA). The MCA sorts each pulse according to its amplitude, which is proportional to the energy of the initial photon, and assigns each pulse to a channel. As pulses, referred to as counts, continue to arrive they are assigned to the appropriate channel depending on the amplitude of the pulse. The final output of the MCA is a channel versus count graph and in order to obtain the desired energy versus count graph, calibration of the detector is required. The detector is calibrated by placing a radioactive isotope source with known energy peaks directly before the detector. Although the temperature drift of the detector was measured to be less than 2% for a temperature change of 10 degrees, and the change of the detector's internal energy calibration due to count rate change was found to be less than 1% when varying the count rates from 800 Hz to 30,000 Hz, the internal energy calibration of the detector can drift by a few percent over several days of operation, which we were unable to eliminate. As a result, the detector is recalibrated for each measured spectrum to avoid errors and two spectra are recorded at each setting: 1) a combined bremsstrahlung and radioactive source spectrum, similar to that shown in Figure 2a, and 2) a pure bremsstrahlung spectrum, similar to that shown in Figure 2b.

The recorded bremsstrahlung spectra are analyzed using a code written in Python [5]. In order to obtain a calibrated bremsstrahlung spectrum the code subtracts the bremsstrahlung spectrum from the combined bremsstrahlung and source spectrum, leaving a radioactive source spectrum as shown in Figure 2c. The subtraction is one-to-one with respect to channel and assumes that the NaI detector's internal energy calibration has not drifted in the short amount of time between recording the combined spectrum and the pure bremsstrahlung spectrum. In order to find the maxima on the radioactive source spectrum's peaks a number of things must be done. First, corrections must be made to the height of each peak since the peak is superimposed on a continuum of background counts. The background counts that appear in the spectra may be due to a number of things, including the radiation emitted from the adjacent Advanced ECR source (AECR), and Compton scatter peaks, plateaus and backscatter peaks resulting from the partial absorption of the bremsstrahlung by the NaI scintillator and surrounding materials. Future work will focus on correcting the spectra for detection efficiencies. The code makes a linear approximation to the background surrounding each peak and subtracts it, as shown in Figure 3. Once the background has been subtracted, a Gaussian fit is applied to the source spectrum peaks. Since there is a large amount of fluctuation in the photon energy emitted by the NaI scintillator for every incident photon energy, a Gaussian fit is appropriate [6]. Due to statistical fluctuations,

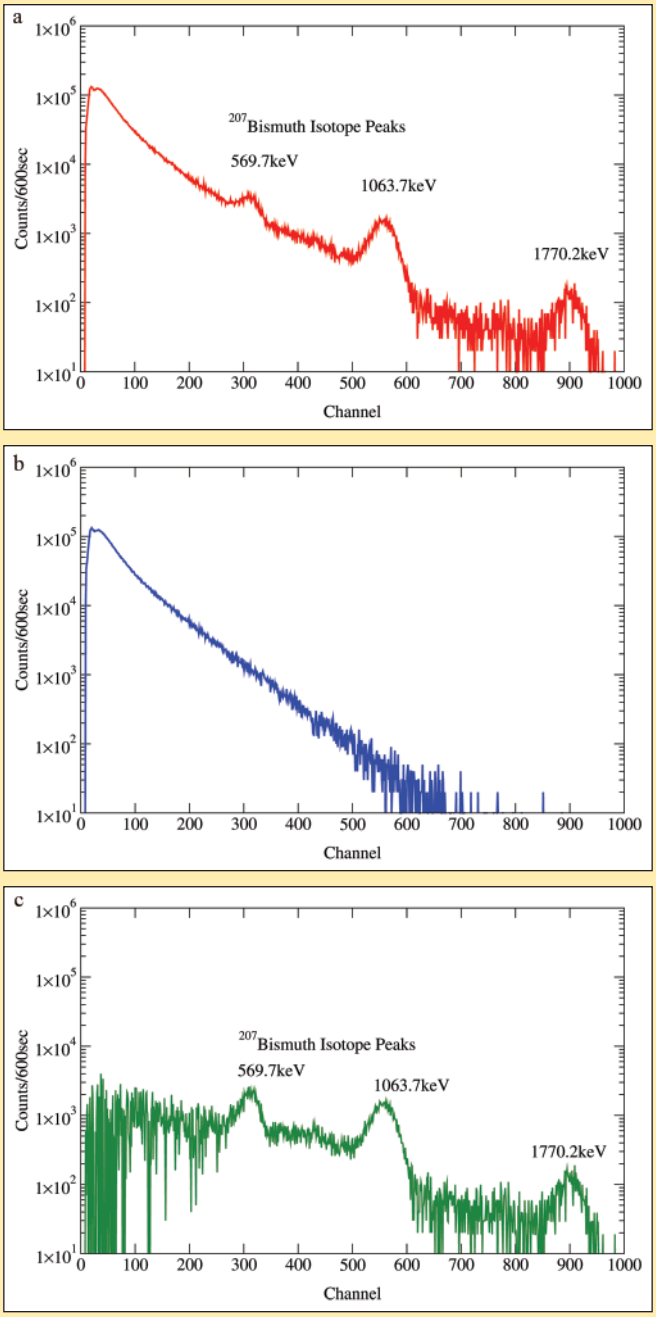

Figure 2. Semi-Logarithmic plots of **(a)** a combined bremsstrahlung and radioactive source spectrum, **(b)** a pure bremsstrahlung spectrum, and **(c)** a pure radioactive source spectrum. The pure radioactive source spectrum is the result of the bremsstrahlung spectrum being subtracted from the combined spectrum.

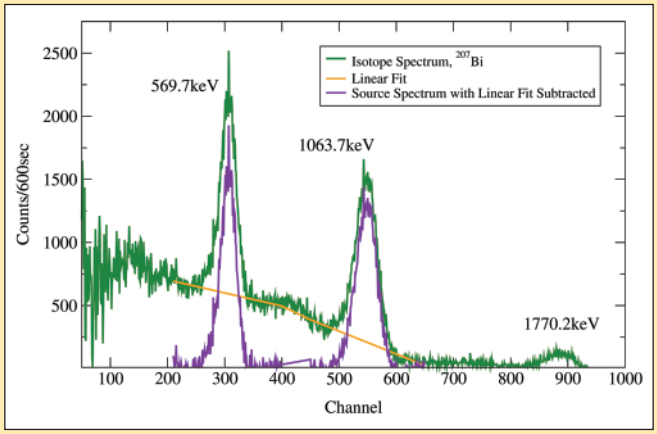

Figure 3. Linear plot of a pure radioactive source spectrum. The Python code calibrates the bremsstrahlung spectrum using the source spectrum. Before determining the peak positions on the source spectrum a linear fit is made to the background and subtracted from it.

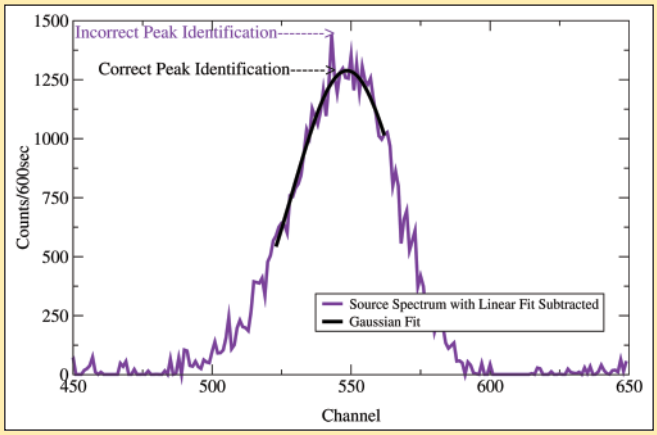

Figure 4. Once the linear approximation to the background is subtracted from the source spectrum a Gaussian fit is applied to the peaks. The Gaussian fit is used to determine the correct position of the peaks.

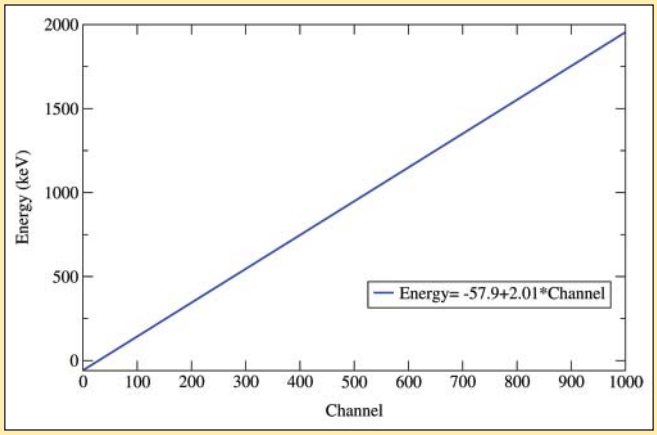

Figure 5. The Python code calibrates the bremsstrahlung spectra. The calibration is a linear relationship between channel and energy as shown here.

simply searching for the channel with the highest count number would lead to an incorrect calibration. Using the Gaussian fit to the peaks, the program finds the correct radioactive source peaks and assigns the appropriate energies to the corresponding channels. An example of an incorrect peak determination and a Gaussian fit used to correctly identify the peak is shown in Figure 4. Since each channel represents an energy value a linear calibration is then obtained, such as shown in Figure 5. The data presented in this paper was calibrated using only the 569.7 keV and 1063.7 keV gamma peaks of Bismuth-207.

Once a spectrum has been calibrated, its spectral temperature, T_S, is obtained. The spectral power, j, emitted is proportional to frequency:

$$j(\omega) \propto \exp[\frac{-\hbar\omega}{kT_S}]$$

where $\hbar$ is Planck's constant, ω is the photon frequency, and k is Boltzmann's constant [7]. Using a semi-logarithmic representation of the data a least-squares fit is applied, from which the inverse of the slope is taken to represent the spectral temperature, T_S. For the spectra discussed in this paper, two energy ranges are used to find T_{S_1} and T_{S_2}: 1) 60–120 keV and 2) 120–200 keV, respectively. In addition to the T_S, the Python code also integrates the spectra for each energy range to give the total counts.

Results

Electron Heating as a Function of Magnetic Field Gradient at Resonance Zone

The plasma is confined by the axial and radial magnetic fields. Together the B_{INJ}, B_{MIN}, and B_{EXT} axial magnetic fields make up the magnetic mirror structure. In order to see the effect that varying one of these parameters has on the hot electron population, the minimum B-Field, B_{MIN}, was varied while B_{INJ} and B_{EXT} were held constant. While B_{MIN} was varied, only 28 GHz heating was used. Using two B_{MIN} values, 0.44 T and 0.70 T, we obtained two $\frac{B_{MIN}}{B_{ECR_{28GHz}}}$ ratios: 1) .44 and 2) .70. The .44 ratio represents a steep magnetic field gradient at the resonant magnetic field surface while a 0.70 ratio

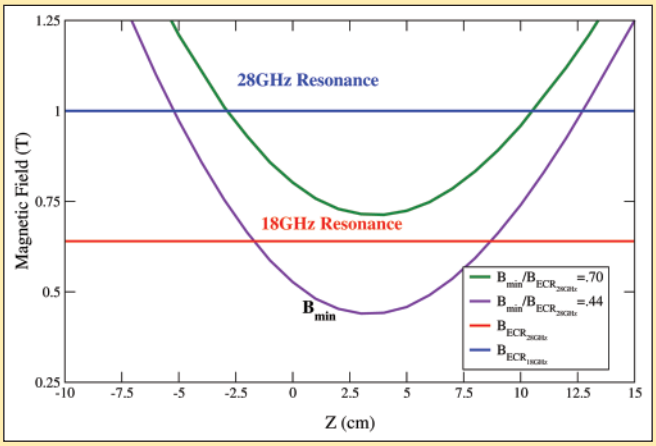

Figure 6. A close look at where the magnetic mirror structures for $\frac{B_{MIN}}{B_{ECR_{28GHz}}}$=.44 and $\frac{B_{MIN}}{B_{ECR_{28GHz}}}$=.70 intersect the 28 GHz resonance zone shows that the .70 ratio has a shallow gradient relative to the steeper .44 ratio.

represents a shallow magnetic field gradient. Figure 6 shows the magnetic mirror structure for these two values and from this figure one can see that the gradient at resonance for a .70 ratio is more shallow than the .44 ratio. Table 1 shows the coil current settings used to produce the magnetic mirror configurations for each ratio. The recorded spectra are shown in Figure 7.

Electron Heating as a Function of Microwave Frequency

In order to see the effect that increased microwave frequency has on the hot electron population, spectra for both 18 GHz and 28GHz were taken at $\frac{B_{MIN}}{B_{ECR_{18GHZ}}}$ and $\frac{B_{MIN}}{B_{ECR_{28GHZ}}}$ ratios of .47 and .70.

.44	Inj	Min	Ext	.70	Inj	Min	Ext
Current (A)	185	153	154	Current (A)	185	113	154
B-Field (T)	3.38	0.44	2.16	B-Field (T)	3.46	0.70	2.23

Table 1. Solenoid current and magnetic field parameters used to compare 28 GHz spectra for $\frac{B_{MIN}}{B_{ECR_{28GHz}}}$ ratios of .44 and .70. The fields B_{INJ} and B_{EXT} are held constant to see the effect varying B_{MIN} has on the hot electron population.

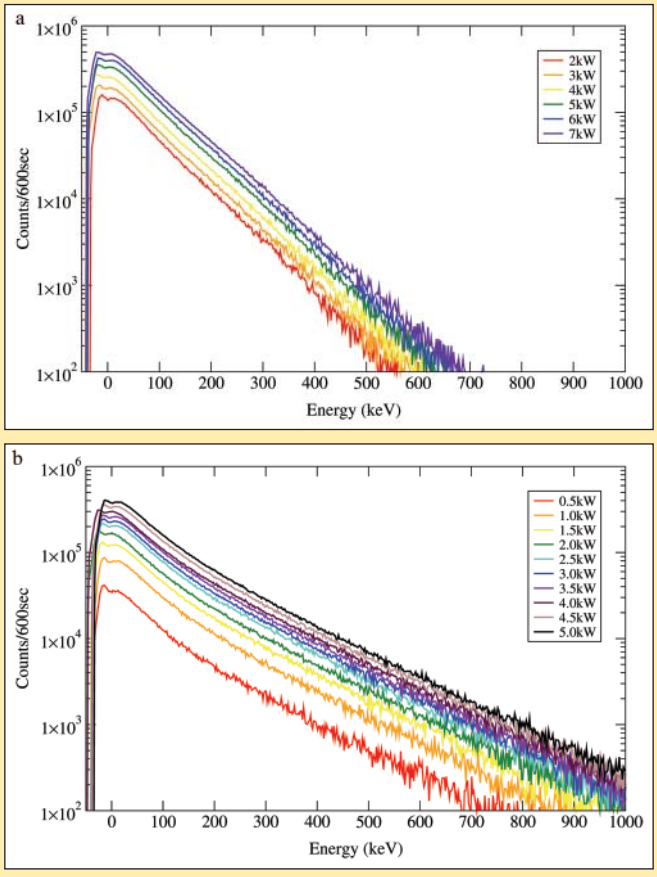

Figure 7. (a) Bremsstrahlung spectra for $\frac{B_{MIN}}{B_{ECR_{28GHz}}}$=.44 with 28 GHz power input varied from 2 kW to 7 kW. **(b)** Bremsstrahlung spectra for $\frac{B_{MIN}}{B_{ECR_{28GHz}}}$=.70 with 28 GHz power input varied from 0.5 kW to 5 kW. The .70 ratio shallow magnetic field leads to more efficient heating since more electrons reach higher temperatures at lower 28 GHz power inputs.

The .70 ratio spectra are shown in Figure 8 and the .47 ratio spectra are shown Figure 9. The 18 GHz spectra are compared to 28 GHz spectra at equivalent ratios. So that the 18 GHz power input remains comparable to the 28 GHz power input in terms of magnetic mirror structure, the 18 GHz current settings used to create the magnetic fields where scaled down by a factor of $\frac{18}{28}$. Table 2 shows the coil current settings used to produce magnetic mirror structures for each ratio at 18 and 28 GHz power inputs.

Discussion and Conclusions

Electron Heating as a Function of Magnetic Field Gradient at Resonance Zone

A comparison of the spectra obtained with steep and shallow gradients, or $\frac{B_{MIN}}{B_{ECR_{28GHZ}}}$ ratios of .44 and .70, respectively, suggests that a shallow gradient at resonance leads to more efficient electron heating. Therefore, higher electron energies can be reached. A shallow gradient allows the electron to remain in the vicinity of the resonance zone for a longer period of time, allowing it to gain more energy. Simulations have shown that the amount of speed gained by an electron in the resonance zone seems to decrease as the square-root of the gradient [8].

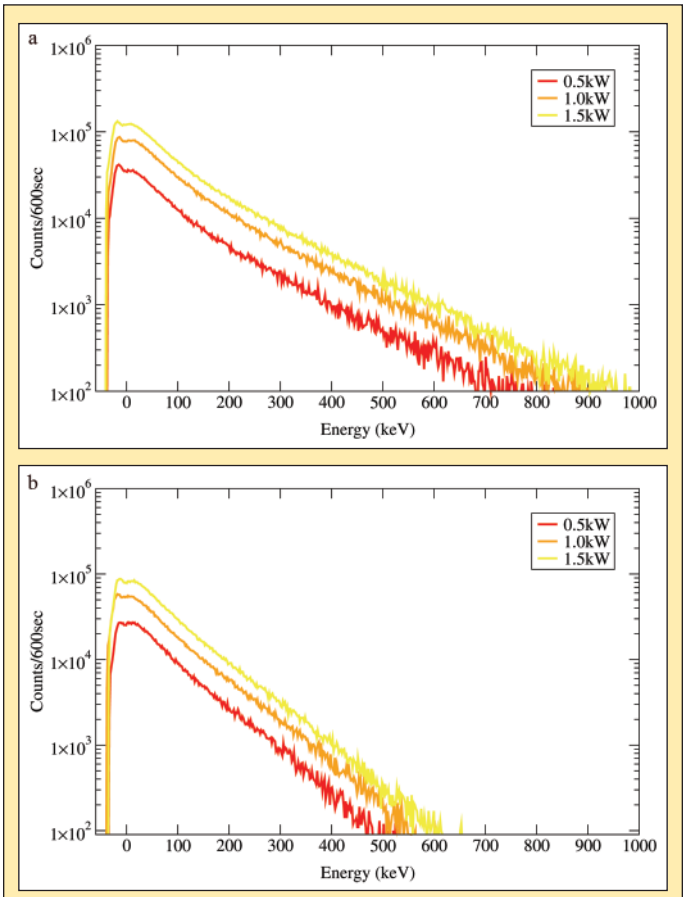

Figure 8. (a) 28GHz bremsstrahlung spectra for $\frac{B_{MIN}}{B_{ECR_{28GHz}}}$=.70. **(b)** 18 GHz bremsstrahlung spectra for $\frac{B_{MIN}}{B_{ECR_{18GHz}}}$=.70. The 18 GHz magnetic fields are scaled down from 28GHz by a factor of $\frac{18}{28}$ in order to achieve equivalent magnetic mirror structures.

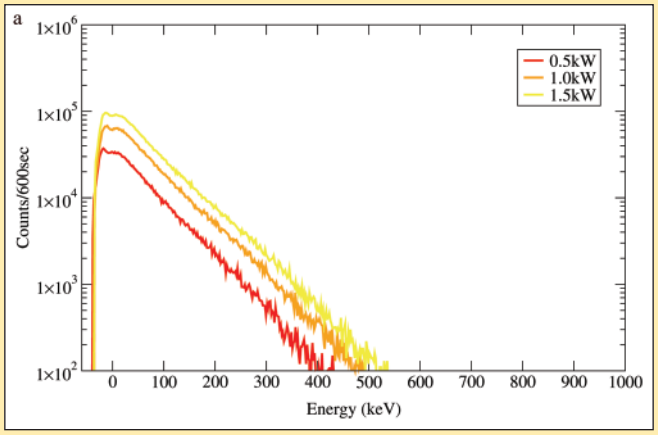

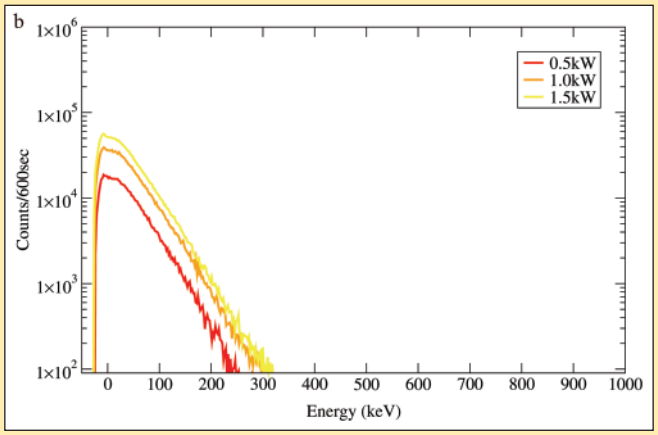

Figure 9. (a) 28 GHz bremsstrahlung spectra for $\frac{B_{MIN}}{B_{ECR_{28GHz}}}$=.47. **(b)** 18 GHz bremsstrahlung spectra for $\frac{B_{MIN}}{B_{ECR_{18GHz}}}$=.47. The 18 GHz magnetic fields are scaled down from 28 GHz by a factor of $\frac{18}{28}$ in order to achieve equivalent magnetic mirror structures.

.44	Inj	Min	Ext	.70	Inj	Min	Ext
28GHz Current (A)	189	158	163	28GHz Current (A)	185	113	154
28GHz B-Field (T)	3.48	0.46	2.29	28GHz B-Field (T)	3.46	0.70	2.23
18GHz Current (A)	122	102	105	18GHz Current (A)	118.6	72.4	98.7
18GHz B-Field (T)	2.23	0.30	1.47	18GHz B-Field (T)	2.22	0.46	1.43

Table 2. Solenoid current and magnetic field parameters used to compare spectra for 18 GHz and 28 GHz heating frequencies. 18 GHz and 28 GHz spectra are recorded for $\frac{B_{MIN}}{B_{ECR}}$ ratios of .47 and .70. The 18 GHz magnetic fields are scaled down from 28 GHz by a factor of $\frac{18}{28}$ for each $\frac{B_{MIN}}{B_{ECR}}$ ratio in order to achieve equivalent magnetic mirror structures.

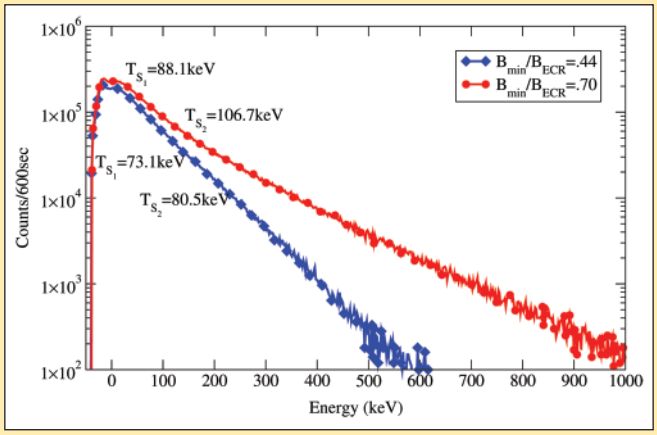

Figure 10. Shown is a direct comparison of a steep magnetic field gradient, $\frac{B_{MIN}}{B_{ECR}}$=.44, and a shallow magnetic field gradient, $\frac{B_{MIN}}{B_{ECR}}$=.70, at equivalent power inputs. The comparison shows that the shallow magnetic field gradient leads to more efficient heating. The spectral temperatures, T_{S_1} (60–120 keV) and T_{S_2} (120–200 keV), for each ratio are indicated and show that electrons present in a shallow magnetic field achieve higher temperatures.

Figure 10 directly compares a .44 ratio spectrum to a .70 ratio spectrum, each at 3 kW of 28 GHz, by indicating the spectral temperature. The spectral temperatures for both ranges, T_{S_1} (60–120 keV) and T_{S_2} (120–200 keV), for the .70 shallow ratio at resonance are greater than the .44 steep ratio by about 17% and 25%, respectively. In addition, the increase in spectral temperature when going from a steep to a shallow magnetic field gradient presents an increased amount of heat deposited onto the cryostat surrounding the plasma chamber. The increase in the amount of heat deposited is supported by the increased counts observed for .70 shallow ratio at each input power, shown in Figure 11. The integrated number of counts for a .70 shallow ratio spectrum is greater by about 50%, or more, at 2 kW of 28 GHz power, and by about 200% at 4 kW of 28 GHz power. These results support simulations which show that electron energy increases with decreasing magnetic field gradient at the resonance zone [9].

Electron Heating as a Function of Microwave Frequency

New generations of ion sources strive for higher microwave frequency capabilities. Since plasma density scales with the square of microwave frequency and magnetic field confinement scales linearly with microwave frequency, higher frequencies are desired [10]. A consequence of increased plasma density at higher frequencies is an increased hot electron population and, as such, an increase in the amount of electrons lost from the plasma. 18 and 28GHz bremsstrahlung spectra recorded for $\frac{B_{MIN}}{B_{ECR}}$ ratios of .47 and .70 show that the difference in emission between 18 and 28 GHz is significant. For both $\frac{B_{MIN}}{B_{ECR}}$ ratios of .47 and .70 the number of hot electrons increases significantly when going from 18 to 28 GHz heating frequencies. This is shown in Figures 8 and 9 where the 28 GHz spectra extend to higher energies.

Figure 12 shows that for a $\frac{B_{MIN}}{B_{ECR}}$ ratio of .70 the spectral temperature does not change when power input is increased. This is also true for the .47 ratio spectral temperatures. As power is increased, the spectrum shape does not change but only shifts upward, suggesting an increase in plasma density, and the slope remains the same, reflecting a constant spectral temperature. Interestingly, when the ratio of 28 GHz to 18 GHz counts is taken for the range 60–120 keV, the .47 ratio case shows a constant increase in counts by a factor of about 2.3 as power input increases, while the .70 case shows an increase in counts by a factor of 1.6. The reason for this remains unclear. Figure 13 shows a direct comparison

between 18 and 28 GHz heating, each at 1.5k W of input power, for both $\frac{B_{MIN}}{B_{ECR}}$ ratios of .47 and .70. For both cases, the spectral temperature in either range increases significantly for 28 GHz heating, indicating an increased hot electron population. These results support simulations which have concluded that electron energy increases with microwave frequency [9].

Concluding Remarks

VENUS, which has already produced record breaking ion beam currents and high charge state distributions, has yet to reach its maximum operating potential. In order to prevent failures as its performance is gradually improved and tested, it is important to take advantage of the diagnostic capabilities the emitted bremsstrahlung can provide. The information provided by the bremsstrahlung is most valuable when accurately analyzed. As such, computer code was developed to extract values such as spectral temperatures and integrated count numbers under various operating conditions. Future work will focus on correcting the spectra for detector efficiencies which may affect these values.

The presented axially emitted bremsstrahlung spectra primarily represent electrons which have been lost from the plasma at the extraction end of the plasma as well as bremsstrahlung emitted from the plasma in the direction of the extraction aperture. Although the axially emitted bremsstrahlung is not an adequate representation of the bremsstrahlung emitted at all surfaces of the plasma, it does give insight into the electron energy distribution of the plasma. The setup of VENUS prevents studies of radially emitted bremsstrahlung, and so an overall determination of the electron losses is not yet known. However, a few conclusions can be drawn from the experimental data obtained. First, a small magnetic field gradient at the electron resonant zone leads to more efficient electron heating. Increasing the power input increases the density of electrons, but has no or very little effect on the electron energy distribution function. Increasing the microwave heating frequency also leads to more efficient electron heating and increases the mean electron energies.

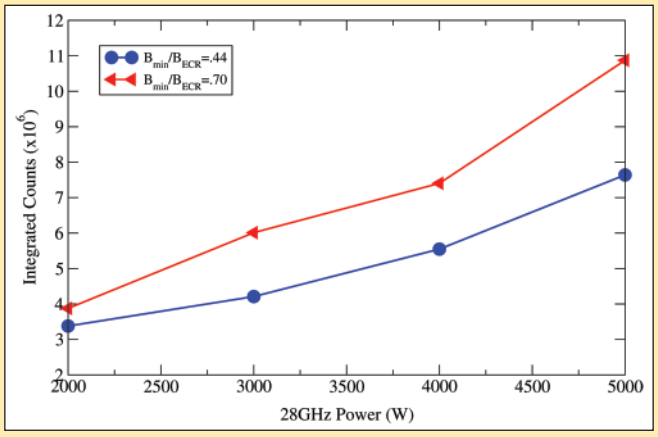

Figure 11. The integrated counts, for the energy range of 60–120 keV, increases with increasing power input as well as with a decreasing magnetic field gradient.

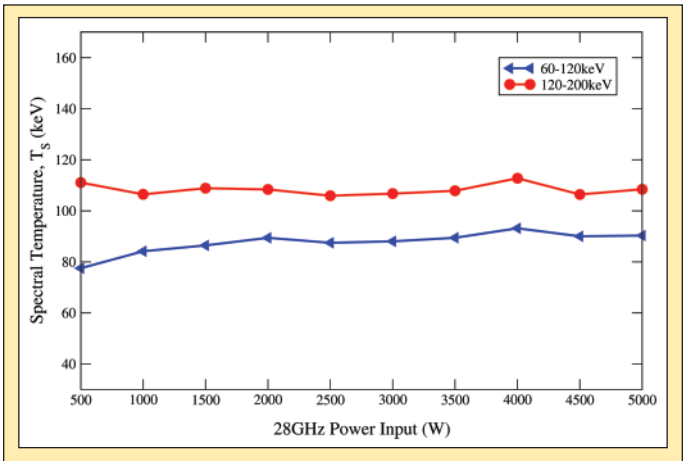

Figure 12. The spectral temperatures, T_{S_1} (60–120 keV) and T_{S_2} (120–200 keV), for a $\frac{B_{MIN}}{B_{ECR_{28GHz}}}$=.70 ratio are shown. As the 28 GHz power input increases the spectral temperature remains constant.

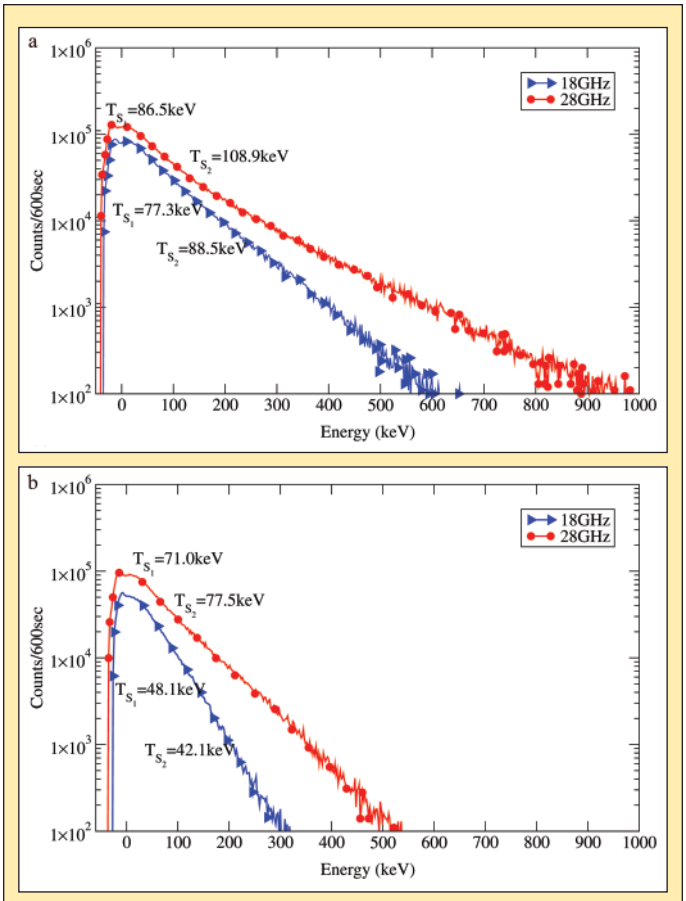

Figure 13. (a) 18 and 28 GHz bremsstrahlung spectra with 1.5 kW power input at $\frac{B_{MIN}}{B_{ECR}}$=.70. **(b)** 18 and 28 GHz bremsstrahlung spectra with 1.5 kW power input at $\frac{B_{MIN}}{B_{ECR}}$=.47. The 18 GHz magnetic fields are scaled down from 28 GHz by a factor of $\frac{18}{28}$ in order to achieve equivalent magnetic mirror structures. The spectral temperatures, T_{S_1} (60–120 keV) and T_{S_2} (120–200 keV), for each heating frequency are indicated.

Acknowledgements

This research was conducted at the Lawrence Berkeley National Laboratory. I thank the U.S. Department of Energy, Office of Science for the opportunity to participate in SULI and experience the process of conducting research. In particular, I would like to thank my mentor Daniela Leitner as well as Damon Todd for their patience and the tremendous amount of time they have spent teaching me how to think like a true researcher. I would also like thank Peggy McMahan for giving me the opportunity to join the 88-inch Group at LBNL, David Ward for his valuable contributions, and my fellow research group members in the ECR group.

REFERENCES

[1] D. Leitner, C.M. Lyneis, T. Loew, D.S. Todd, S. Virostek, and O. Tarvainen, "Status Report of the 28GHz Superconducting Electron Cyclotron Resonance Ion Source VENUS," *Review of Scientific Instruments*, vol. 77, 03A302, February 2006.

[2] C. Lyneis, D. Leitner, D. Todd, S. Virostek, T. Loew, A. Heinen, and O. Tarvainen, "Measurement of Bremsstrahlung Production and X-Ray Cryostat Heating in VENUS," *Review of Scientific Instruments*, vol. 77, 03A342, March 2006.

[3] C. Barue, M. Lamoureux, P. Briand, A. Girard, and G. Melin, "Investigation of hot electron-cyclotron resonance ion sources," *Journal of Applied Physics*, vol. 76, no. 5, September 1994.

[4] D. Leitner, C.M. Lyneis, S.R. Abbott, D. Collins, R.D. Dwinell, M.L. Galloway, M. Leitner, and D.S. Todd, "Next Generation ECR ion sources: First Results of the superconducting 28 GHz ECRIS-VENUS," *Nuclear Instruments and Methods in Physics Research B*, vol. 235, 486–496.

[5] "Python Programming Language-Official Website," [cited 2007 Aug 09], http://www.python.org/.

[6] G. F. Knoll, *Radiation Detection and Measurement, 2nd Edition*, New York: John Wiley & Sons, Inc., 1989: 114–117.

[7] R. Geller, *Electron Cyclotron Resonance Ion Sources and ECR Plasmas*, Bristol: Institute of Physics Publishing, 1998: 252.

[8] Y. Jongen. "E.C.R. Electron Acceleration", *Proceedings of the Sixth International Workshop on ECR Ion Sources*, January 17th–18th, 1985, Berkeley, California, USA.

[9] H. Koivisto, "The effect of microwave frequency and grad B on the energy of electrons in an electron cyclotron resonance ion source," *Review of Scientific Instruments*, vol. 70, no. 7, July 19.

[10] D. Leitner and C.M. Lyneis, "ECR Ion Sources," *The Physics and Technology of Ion Sources, 2nd Edition*, Ian G. Brown (ed.), Weinheim: Wiley-VCH, 2004: 203–227.